

Nanoscale Fabrication of Microwave Detectors from Commercially-Available CVD-Grown Monolayer Graphene

Michael R. Gasper^{*}, Ryan C. Toonen^{*}, Nicholas C. Varaljay[†], Robert R. Romanofsky[‡], Félix A. Miranda[‡]

^{*} Department of Electrical and Computer Engineering
University of Akron, Akron, OH, 44325 USA

[†] Space Environment Test Branch

NASA-Glenn Research Center, Cleveland, OH 44135

[‡] Communications and Intelligent Systems Division

NASA-Glenn Research Center, Cleveland, OH 44135

Abstract—Using commercially-available monolayer graphene, synthesized by means of chemical vapor deposition, microwave power sensing elements have been nanofabricated and integrated with microwave-grade test structures suitable for on-wafer probing. The graphene, situated on a thermal oxide, was first cleaned of stray contaminants in a forming gas environment briefly held at 250 degrees Celsius using a rapid thermal annealer. Immediately following this step, the graphene was passivated with a protective aluminum oxide layer (approximately 5 nm in thickness). Micrometer-scale Corbino disc test structures were then fabricated in direct contact with the graphene using a self-aligned process, which relies on the fact that tetramethylammonium hydroxide develops the photoresist while removing the aluminum oxide. Graphene nanoribbons (with widths as small 400 nm) were then fabricated across the Corbino disc gaps using electron-beam writing in conjunction with a negative tone resist. The same developer exposed the majority of the graphene while defining nanometer-scale lines of photoresist stacked upon aluminum oxide. These stacks served as etch-stops while the unprotected graphene was ion-milled in an oxygen plasma. Finally, the photoresist was removed leaving behind passivated graphene nanoribbons. Damage caused by the fabrication was evaluated by comparing the Raman spectra of the graphene before and after processing.

Index Terms—Graphene, detectors, microwave measurements, Corbino disc, nanowire, lithography, electron beam.

I. INTRODUCTION

Graphene, a single atom layer of carbon in a hexagonal lattice, is of great interest in radio frequency and microwave applications due to its high carrier mobility and DC transfer characteristic [1]. The chemical vapor deposition (CVD) technique for synthesizing graphene is relatively inexpensive, allows for large-scale production, and enables graphene to be transferred to a variety of microwave-compatible substrates. In this paper we discuss the details involved in our simple, single-lithography-mask approach for making microstructures that have a Corbino disc geometry [2] with a back gate for modulating channel conductance [3] and details on our electron beam lithography process for writing nanoribbons within the Corbino disc microstructures.

II. MICROFABRICATION OF CORBINO DISCS

Work has been done in order to improve the previously reported device processing method [4]. Fig. 1 outlines the Corbino disc test structure fabrication process. The process starts by first cleaning commercially available, CVD-grown monolayer graphene on silicon dioxide/silicon (SiO₂/Si) [5] with rapid thermal annealing (RTA) in forming gas (nitrogen with 4.5% hydrogen) atmosphere at 250 °C for 12 minutes. The RTA helps to reduce impurities absorbed by the graphene surface [5]. Then, a 5 nm sacrificial layer of aluminum was deposited over the entire substrate and allowed to form a native oxide passivation layer. This complete metal covering was used to protect the graphene during photolithographic processing. The RTA clean and passivation layer desposition is necessary in order to protect the graphene layer during device processing and prevent exposure to ambient air.

A protective layer of positive photoresist, AZ4210, was spun over the top of the sample at 500 rpm for 3 s followed by 3000 rpm for 42 s and hard baked for 30 minutes at 95 °C. The sample was then immersed in a buffered oxide etchant, 1:1 :: (6:1 BOE):dionized water, for 6 minutes to remove the back layer of SiO₂, a necessary step to allow for contact to the back gate. Remaining photoresist was removed with acetone and the Al-oxide passivation layer remains on top of the graphene preventing degradation of the graphene surface when exposed to potential contaminants.

Adhesion promoter was spun on the sample at 500 rpm for 3 s followed by 3000 rpm for 42 s and baked on a hotplate at 180 °C for 8 minutes. Negative photoresist, AZnLOF 2020 diluted with AZ edge bead remover in a 1:1 ratio [6], [7], was spun on the sample at 500 rpm for 3s followed by 3500 rpm for 42 s. The diluted resist spun to a thickness of 400 nm. The edge bead was removed using AZ edge bead remover and the samples were soft baked at 110 °C for 15 s. The samples were subsequently exposed at an intensity of approximately 15 mW/cm² for 1.5 s with a subsequent post exposure bake on a hotplate at 110 °C for 3 minutes. The samples was

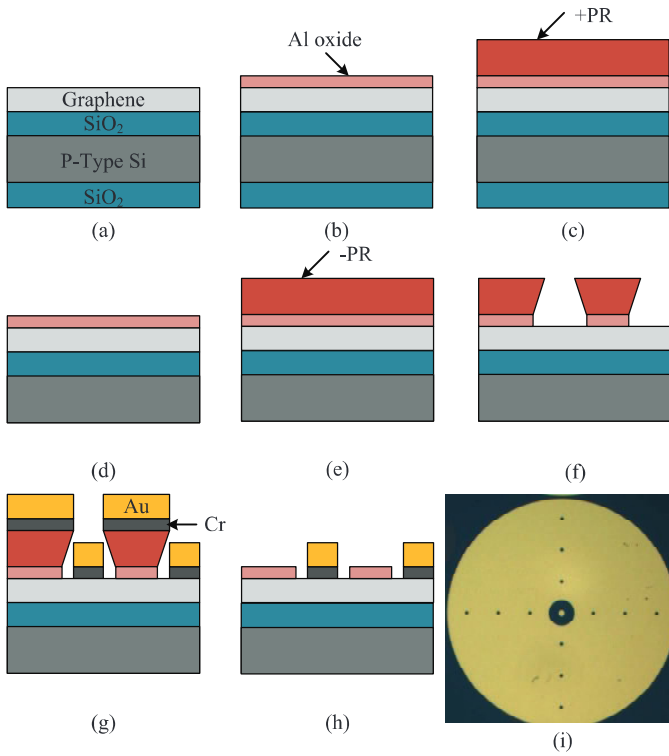


Fig. 1. (a) RTA cleaned graphene on Si substrate with SiO₂ thermal oxide. (b) Metallization of sacrificial aluminum layer. (c) Spin on positive photoresist for BOE. (d) removal of back SiO₂ oxide with BOE. (e) Spin on negative photoresist for microlithography. (f) Pattern with negative photomask. (g) Metallization of Cr/Au contact layer. (h) Lift-off excess photoresist and metal. (i) Photo of finished Corbino disc test structure.

developed in AZ300 MIF for 15 s. The chosen developer not only patterned the photoresist but also selectively etched away the aluminum oxide layer [8]. A 5 nm layer of chromium (Cr) and 50 nm layer of gold (Au) was deposited via e-beam evaporation for electrical contact. Lift-off was done with Remover PG stripper at 70 °C for approximately 2 hours to finalize the Corbino structure. Fig. 1 shows a diagram of the process flow. It is critical to use a stripper that does not attack aluminum during the lift-off process. The aluminum oxide passivation must remain to protect the graphene layer for subsequent nano-processing. This microfabrication process has a device yield of nearly 70%.

The Raman spectra were collected before and after processing the sample. The spectrum before microfabrication is of the graphene passivated with aluminum oxide. Characteristic G and G' peaks are present. The aluminum interferes with the spectrum of the graphene and does not show monolayer at this time. The spectrum collected after microfabrication, on unpassivated patches, shows the the graphene remained intact and is monolayer, Fig. 2, [9]. Some defects were created on the graphene during the device processing as shown by the D band peak ($\sim 1350\text{ cm}^{-1}$) on the Raman spectrum [10].

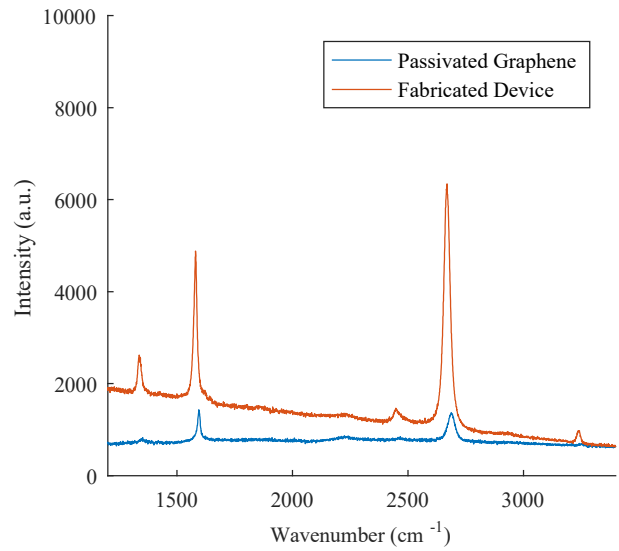


Fig. 2. Raman spectrum of the passivated sample before device processing and spectrum of the sample after the microfabrication process.

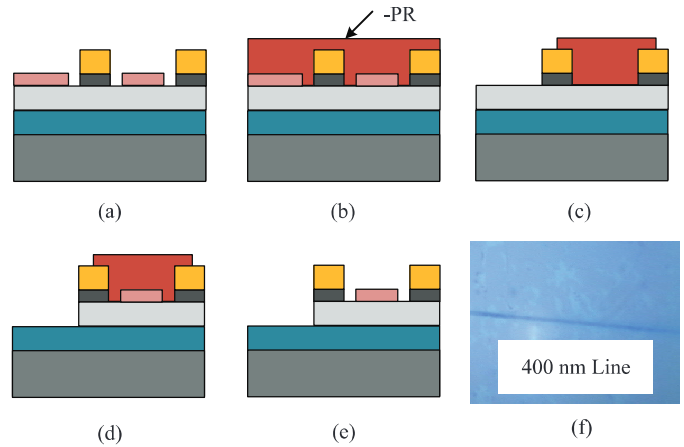


Fig. 3. (a) Graphene Corbino discs from microfabrication process. (b) Spin on negative photoresist for EBeam writing. (c) Pattern nanoribbons in Corbino disc gap. (d) Ion milling of exposed graphene. (e) Strip remaining photoresist. (f) Photo of finished Corbino disc test structure with nanoribbons.

III. GRAPHENE NANORIBBON FABRICATION

Nano-scaled lines were etched into the graphene between the microfabricated Corbino disc structures. The same diluted negative photoresist used in the microfabrication was spun on top of the Corbino disc structures following adhesion promoter. Electron beam writing was done with a Hitachi... SEM outfitted with a Naby Nanopattern Generation System. The electron beam lithography was aligned to the microstructures in order to pattern lines with widths down to... in between the Corbino disc contacts, Fig. 3. The samples were exposed to a dose of $13\ \mu\text{C}/\text{cm}^2$ at a beam current of 20.7 pA with a working distance of approximately 11 mm.

After ebeam writing the sample was developed in AZ300MIF for 15 s. The patterned photoresist served as etch-

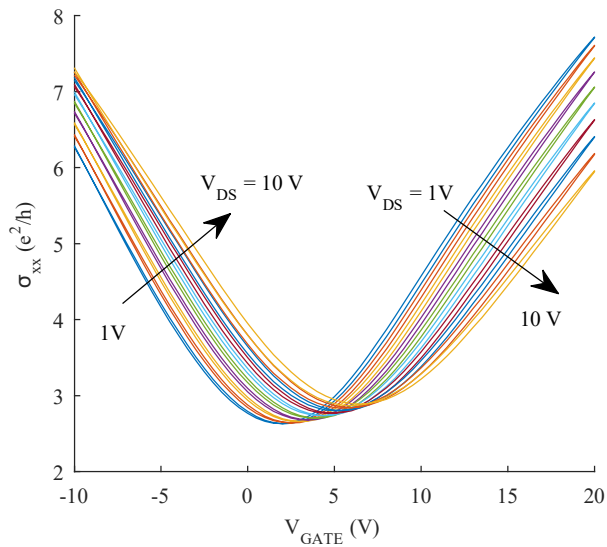


Fig. 4. Conductivity vs gate voltage for V_{DS} varied between 1 V and 10 V and displaying a charge neutrality point between 2 V and 6 V. ***Temporary Placeholder Until Data is Collected***

stops while the unprotected graphene and remaining aluminum oxide was ion-milled in an oxygen plasma for 5 s at a power of 5 W. Finally, the photoresist was removed leaving behind passivated graphene nanoribbons. Strict timings during the development and etching steps reduce device yield.

IV. ELECTRICAL MEASUREMENTS ***WORK IN PROGRESS***

DC current vs voltage traces were collected to verify continuity of the nanowire between the contacts of the Corbino discs. Device drain-source (inner disc-outer disc) current versus gate voltage for varying bias voltages was collected using a Keithley 4200 SCS, Fig 4. The graphene nanoribbons have been used to realize a microwave power detector operating at 433.92 MHz, in the ISM band. The devices were fed with incident microwave power chopped at approximately 1.5 kHz (1501.487 Hz). A voltage measurement was taken via lock-in detection at the chopping frequency on the device under test. An illustration of the experimental structure is shown in Fig. 5 [4]. Preliminary data shows a power sensitivity of ***Data must be collected***.

V. CONCLUSIONS

Our simple one mask microfabrication process has a device yield of nearly 70%. However, final steps in the nanofabrication process reduce this high yield. The final development etches the remaining aluminum oxide but can also undercut the nano-patterned lines and remove the structures. The ion-milling step may also result in damaged devices. Work must be done to optimize these two final process steps. The developer may be diluted to offer more latitude in the timing before undercutting the oxide and removing structures. The timing and gas composition of the reactive ion etch may also be

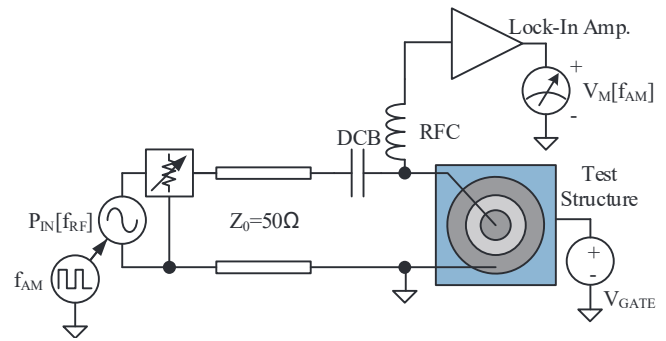


Fig. 5. Schematic of the graphene power detection circuit.

optimized to better attack the aluminum oxide while leaving the photoresist layer intact.

ACKNOWLEDGMENT

The authors would like to thank Dr. Zhorro Nikolov and the National Polymer Innovation Center at the University of Akron for assistance with Raman Spectroscopy.

REFERENCES

- [1] T. Palacios, A. Hsu, and H. Wang, "Applications of graphene devices in rf communications," *IEEE Communications Magazine*, vol. 48, no. 6, pp. 122–128, June 2010.
- [2] C. Stellmach, A. Hirsch, G. Nachtwei, Y. B. Vasilyev, N. Kalugin, and G. Hein, "Fast terahertz detectors with spectral tunability based on quantum hall corbino devices," *Applied Physics Letters*, vol. 87, no. 13, p. 133504, 2005.
- [3] A. B. Fowler, F. F. Fang, W. E. Howard, and P. J. Stiles, "Magneto-oscillatory conductance in silicon surfaces," *Physical Review Letters*, vol. 16, no. 20, p. 901, 1966.
- [4] M. R. Gasper, N. Parsa, and R. C. Toonen, "Microwave power detection with gated graphene," in *2017 IEEE 17th International Conference on Nanotechnology (IEEE-NANO)*, July 2017, pp. 118–120.
- [5] Graphenea monolayer graphene film on various substrates. graphenea, inc. [Online]. Available: <https://www.graphenea.com/>
- [6] E. Herth, E. Algret, P. Tilmant, M. Francois, C. Boyaval, and B. Legrand, "Performances of the negative tone resist aznlof 2020 for nanotechnology applications," *IEEE Transactions on Nanotechnology*, vol. 11, no. 4, pp. 854–859, 2012.
- [7] B. R. Romanczyk, *Fabrication and characterization of III-V tunnel field-effect transistors for low voltage logic applications*. Rochester Institute of Technology, 2013.
- [8] A. Hsu, H. Wang, K. K. Kim, J. Kong, and T. Palacios, "Impact of graphene interface quality on contact resistance and rf device performance," *IEEE Electron Device Letters*, vol. 32, no. 8, pp. 1008–1010, Aug 2011.
- [9] Z. Ni, Y. Wang, T. Yu, and Z. Shen, "Raman spectroscopy and imaging of graphene," *Nano Research*, vol. 1, no. 4, pp. 273–291, 2008. [Online]. Available: <http://dx.doi.org/10.1007/s12274-008-8036-1>
- [10] L. G. D. Arco, Y. Zhang, A. Kumar, and C. Zhou, "Synthesis, transfer, and devices of single- and few-layer graphene by chemical vapor deposition," *IEEE Transactions on Nanotechnology*, vol. 8, no. 2, pp. 135–138, March 2009.